


 Cite this: *RSC Adv.*, 2021, 11, 27092

Green synthesis of gold nanoparticles from *Manilkara zapota* L. extract and the evaluation of its intrinsic *in vivo* antiarthritic potential†

 Mahnoor Ijaz,‡^a Maryam Fatima,‡^b Rukhsana Anwar*^b and Maliha Uroos ^{*a}

The plant *Manilkara zapota* belongs to the family Sapotaceae and is commonly known as Chiku in Pakistan. Traditionally, *M. zapota* is used in pulmonary diseases, diarrhea, rheumatism, hemorrhage, and ulcers. There is no study available on the *in vivo* antiarthritic activity of *M. zapota* and its gold nanoparticles (AuNPs). The aim of this study is to evaluate the *in vivo* acute and sub-acute antiarthritic activity of aqueous extract of *M. zapota* and its biosynthesized gold nanoparticles (AuNPs). Plant-induced reduction method was used for the synthesis of AuNPs. The synthesized AuNPs were characterized *via* UV, FTIR, SEM, and zeta potential measurements and were optimized by screening various parameters including time, temperature, pH, and salt concentration. Arthritis in rats was induced by Freund's Complete Adjuvant (FCA) injection in hind paw. The antiarthritic effect was evaluated by the determination of paw volume, joint diameter, latency time, hematological, biochemical parameters, antioxidant biomarkers, TNF- α level, and radiological evaluation. The aqueous extract and nanoparticles significantly decreased the paw volume, joint diameter, and significantly increased latency time as compared to the FCA-induced arthritic group. They significantly normalized the hematological, biochemical parameters, and oxidative stress biomarkers in comparison to the arthritic group. They also significantly decreased the TNF- α level when assessed against the arthritic group. Radiological evaluation confirmed the antiarthritic effect of the aqueous extract and nanoparticles of *M. zapota* leaf extract. It is concluded that the aqueous extract and nanoparticles of *M. zapota* possess significant analgesic, antiarthritic, and anti-inflammatory activity. However, nanoparticles possess more pronounced antiarthritic activity as compared to the aqueous extract. Moreover, free radical scavenging action and TNF- α reduction showed a prominent role in their antiarthritic activity. Further, investigation is underway to identify the active phytochemical constituent responsible for the antiarthritic activity.

Received 23rd April 2021

Accepted 15th July 2021

DOI: 10.1039/d1ra03186d

rsc.li/rsc-advances

Introduction

Rheumatoid arthritis (RA) is a chronic, systemic inflammatory, and autoimmune disorder, which is characterized by the uncontrolled proliferation of the synovial tissue and a wide array of multisystem comorbidities. A complex interplay between environmental and genetic factors is responsible for rheumatoid arthritis.¹ Rheumatoid arthritis patients not only have pain, swelling, stiffness, and joint damage but also have a disability. Generally, the treatment for rheumatoid arthritis consists of NSAIDs glucocorticoids and disease-modifying

antirheumatic drugs (DMARDs).^{2,3} In rheumatoid arthritis, various enzymes leak out from the liver and the elevation of their levels in blood occurs. Reactive oxygen species (ROS) produced by phagocytic cells such as neutrophils and macrophages along with hypoxia and reoxygenation lead to chronic oxidative stress in the RA synovial tissue. The generated ROS could damage the nucleic acids, lipids, proteins, and matrix components.⁴

Manilkara zapota L. belongs to the family Sapotaceae, which includes about 700 species and 40 genera. "Sapodilla" is derived from the Spanish word "zapotilla", which means sapote (a soft edible fruit). Sapodilla is distributed globally, and is native to tropical America and Southern Mexico. Traditionally, the decoction of young fruits of *M. zapota* was employed as anti-diarrhea, diuretic, aperients (laxative), febrifuge, and tonic. The decoction of leaves was used in cough, fever, cold, and diarrhea. The crushed powder of the seeds was frequently applied to expel kidney and bladder stones.⁵ *M. zapota* has been investigated for its antioxidant activity.⁶ The anticancer potential of sapodilla fruits that contain 4-*O*-galloylchlorogenic acid and methyl 4-*O*-

^aCentre for Research in Ionic Liquids, School of Chemistry, University of the Punjab, Quaid-e-Azam Campus, 54590 Lahore, Pakistan. E-mail: malihauroos.chem@pu.edu.pk

^bPunjab University College of Pharmacy, University of the Punjab Lahore, Pakistan. E-mail: rukhsana.pharmacy@pu.edu.pk

† Electronic supplementary information (ESI) available. See DOI: 10.1039/d1ra03186d

‡ Joint first authors.



galloylchlorogenic acid have been examined in colon cancer cells.⁷ The stem, bark, and leaves of *M. zapota* have been investigated for their antimicrobial activities against some pathogenic bacteria and fungi.⁸ The hypoglycemic activity in leaves, roots, and seeds extracts of *M. zapota* is due to the occurrence of many phytochemicals.⁹ The plant leaves have anti-inflammatory activity as *M. zapota* contains compounds such as steroids (glycosides, cardiac glycosides), terpenoids, and flavonoids.¹⁰ *M. zapota* possess an antinociceptive activity and antidiarrheal activity due to the presence of flavonoids, alkaloids, terpenes, sterols, sugars, saponins, and alkaloids.¹¹ *M. zapota* showed a significant *in vitro* protection against the denaturation of proteins, which shows that it could be used as an antiarthritic agent in the future.¹²

Nanoparticles are the simplest structures with a size range in nanometer (nm). A group of atoms with structural radius < 100 nm is considered as nanoparticles.¹³ The word “nano” is derived from the Greek language word “nanos” meaning “tiny”, very small, or “dwarf”.¹⁴ Using the plant extract, the synthesis of nanoparticles offers an alternative, inexpensive, efficient, and environment friendly method, and provides an alternative route to use natural ingredients in plant extracts.^{15,16} Gold nanoparticles (AuNPs) are a promising class of nanomaterials that are inert in the biological environment. They have physical properties that are suitable in various biomedical applications including therapeutic and diagnostic applications. Silver nanoparticles of *M. zapota* extracts have been used in antimicrobial activity,¹⁷ showing deterrent activity on *M. domestica*¹⁸ and acaricidal activity.¹⁹ Among various animal models for the induction of arthritis, Freund's Complete Adjuvant (FCA) has been widely used in rats because it shows reliable onset, easily measurable, exhibits robust progression, induces polyarticular inflammation, encourages bone proliferation, and prompts marked bone resorption.²⁰ The present study was designed to evaluate and compare the *in vivo* analgesic, antiarthritic and anti-inflammatory activities of the aqueous extract of *Manilkara zapota* and its respective biosynthesized gold nanoparticles.

Experimental

Materials

Indomethacin capsules (Munawar Pharma PVT Ltd), diclofenac sodium tablets (Novartis Pharma PAK Ltd), carrageenan (M/s Bio Basic, Canada), Freund's Complete Adjuvant (M/s Sigma Aldrich, St. Louis USA), 1-Chloro-2,4-dinitrobenzene (CDNB), pyrogallol, sodium chloride, and tetramethylpropane (TMP) were supplied by Sigma Aldrich Co. Ltd, Korea. Di-sodium hydrogen phosphate, hydrochloric acid, potassium dichromate, and sodium potassium tartrate were supplied by Reidel_deHaen, Sigma Aldrich. Copper sulfate pentahydrate, hydrogen peroxide, potassium dihydrogen phosphate, and reduced glutathione (GSH) were supplied from Merck, Germany. For alkaline phosphatase (AP), alanine transaminase (ALT), and aspartate transaminase (AST) analysis kits by Crescent Diagnostics were used. For TNF- α analysis, a kit by Glory Science Co., Ltd was used.

Collection of plants and preparation of the plant extract

Fresh leaves of *Manilkara zapota* L. were collected from Lahore, Punjab in the month of May. Botanical identification and authentication of plant leaves was carried out by Dr Zaheer-ud-Din Khan, a taxonomist at the Department of Botany, GC University, Lahore. He issued a voucher number (GC. Herb. Bot. 3504) for the plant and the voucher specimen was deposited at the Herbarium Department GC University, Lahore for future reference. The leaves were separated from twigs, made free from dirt, and dried under shade for two weeks. The dried leaves were then crushed to powder. The extraction of the powdered leaves was made by maceration with distilled water. The yield obtained for the aqueous extract was 5.7%.

Synthesis of gold nanoparticles (AuNPs) from the leaf extract

6 mL of yellow-colored $\text{HAuCl}_4 \cdot 3\text{H}_2\text{O}$ was taken in a beaker. Sodium bicarbonate was added in this solution to neutralize it. Then, 1 mL aqueous extract was added in it and the solution was stirred in dark for 10 minutes at room temperature. The color of the solution was changed to purple immediately. The reaction mixture was monitored by a UV-Vis spectrophotometer. In order to study the stability of the AuNPs formed, the UV spectra of the reaction mixture was taken after every 24 hours until 18 days.

Study of different factors affecting the synthesis of gold nanoparticles

The biosynthesis of AuNPs was carried out with changing concentration of the leaf extract. The effect of aqueous leaf extract concentration on the biosynthesized AuNPs was studied by carrying out the reaction at 0.25, 0.5, 2, 4, 6, 8, and 10% leaf extracts. The effect of temperature on the synthesis rate and the particle size/shape of the prepared AuNPs was studied by carrying out the reaction at 0, 60, 80, and 100 °C with continuous stirring. The biosynthesis of AuNPs was carried out at the pH of 1, 3, 5, 7, and 9 with continuous stirring. In order to study the effect of the salt on the stability of biosynthesized AuNPs, an equal amount of the AuNPs reaction mixture was treated with varying concentrations of NaCl solution including 1, 2, 3, 4, and 5 M. The synthesis of AuNPs was also investigated at different time intervals between 2 and 16 minutes.

Characterization of the synthesized AuNPs

The AuNPs synthesized by the green approach were characterized for their optical properties using a UV-Vis spectrophotometer (T90, PG Instruments Ltd). The functional group analysis for the reduction of Au^{3+} ions, resulting in formation of AuNPs, was done using an FT-IR spectrophotometer (Cary 630, Agilent Technology, USA within the spectral range of 4000–625 cm^{-1}). The purified AuNPs were freeze dried, and their structure and composition were analyzed by scanning electron microscopy (SEM). To determine the nature and size of the synthesized AuNPs, X-ray diffraction (XRD) and zeta potential studies were performed.



Experimental animals

Female Sprague Dawley rats were obtained from the University of Veterinary and Animal Sciences (UVAS), Lahore, Pakistan. All protocols were approved by the Animal Ethics Committee of Punjab University College of Pharmacy (PUCP), University of Punjab Lahore, Pakistan (approval voucher no: AEC/PUCP/1097) for the purpose of control and supervision of experiments on animals.

Housing of animals

Animals were housed in a separate room of animal house of PUCP, Allama Iqbal, Campus, Lahore. They were kept in steel and polypropylene cages and were acclimatized for a period of about two weeks. Animals were maintained under controlled conditions (25 ± 2 °C), with relative humidity of 45–55% and 12 : 12 light–dark cycle. They were provided with standard diet and water *ad libitum*.

Experimental protocol

Total 64 healthy adult Female Sprague Dawley (SD) rats weighing (130–200 g) were randomly selected for this experimental protocol from Animal House PUCP, Allama Iqbal, Old Campus, Lahore. Rats were divided into two groups. Each group consisted of 32 rats. One group was selected for the acute study and other for the sub-acute study. The aqueous extract and gold nanoparticles of *M. zapota* leaf extract were used for both acute and sub-acute studies. The aqueous extract of *M. zapota* was labeled as AEMZ and the gold nanoparticles were labeled as Gold NPMZ.

Experimental protocol for acute study

One group of SD rats was divided into 8 sub-groups of four animals in each as follows.

Negative control: administered vehicle only, 1 h before carrageenan injection.

Positive control group: administered diclofenac sodium (100 mg kg^{-1}) orally, 1 h before carrageenan injection.

AEMZ 200 mg kg^{-1} group: administered aqueous extract of *M. zapota* (200 mg kg^{-1}) orally, 1 h before carrageenan injection.

AEMZ 400 mg kg^{-1} group: administered aqueous extract of *M. zapota* (400 mg kg^{-1}) orally, 1 h before carrageenan injection.

Gold NPMZ 4 mg kg^{-1} group: administered biosynthesized gold nanoparticles of *M. zapota leaf extract* intraperitoneally, 1 h before carrageenan injection.

Gold NPMZ 5 mg kg^{-1} group: administered gold nanoparticles of *M. zapota leaf extract* intraperitoneally, 1 h before carrageenan injection.

In the rats, edema was induced by an injection 0.1 mL of 1% (w/v) of carrageenan in saline in to sub-plantar region of the left hind paw. The edema volumes in the control and treated groups with the standard drug and extracts were noted at respective time intervals and the percentage inhibition of paw edema was calculated by the following formula.

% paw edema inhibition

$$= \frac{(E_t - E_o)_{\text{control group}} - (E_t - E_o)_{\text{treated group}}}{(E_t - E_o)_{\text{control group}}} \times 100$$

where E_o is the paw volume at zero time before carrageenan injection, E_t is the paw volume at the respective time, and $(E_t - E_o)$ is the paw edema.

Experimental protocol for sub-acute study

Freund's Complete Adjuvant (FCA) induced chronic arthritis. The SD rats were divided into 8 groups of four animals each as follows.

Normal control: administered distilled water till 28 days.

Arthritic control: arthritis was induced in rats with FCA.

Positive control group: administered indomethacin (4 mg kg^{-1}) orally once daily, from the 12th day till the 28th day after FCA induction.

AEMZ 200 mg kg^{-1} group: administered aqueous extract of *M. zapota* (200 mg kg^{-1}) orally once daily, from the 12th day till the 28th day after FCA induction.

AEMZ 400 mg kg^{-1} group: administered aqueous extract of *M. zapota* (400 mg kg^{-1}) orally once daily, from the 12th day till the 28th day after FCA induction.

Gold NPMZ 5 mg kg^{-1} group: administered gold nanoparticles of *M. zapota* leaf extract (0.6 mg) intraperitoneally once daily, from the 12th day till the 28th day after FCA induction.

Experimental arthritis was induced in rats with 0.1 mL of Freund's complete adjuvant (FCA) injection into the sub-plantar region of the left hind paw on the day. The dosing of all the groups started from day 12 once daily.

Behavioral assessment

Paw volume. The left hind paw volumes of all the rats were measured at 0 day before the induction of FCA and thereafter, on day 4, 8, 12, 16, 20, 24, and day 28 using a plethysmometer and the percentage inhibition of paw edema was calculated by the following formula.

$$\% \text{ paw edema inhibition} = \frac{(E_t - E_o)_{\text{FCA group}} - (E_t - E_o)_{\text{treated group}}}{(E_t - E_o)_{\text{FCA group}}} \times 100$$

where E_o is the paw volume at zero day before FCA injection, E_t is the paw volume at the respective day, and $(E_t - E_o)$ is the paw edema.

Joint diameter. The left hind paw joint diameters of all the rats were measured at 0 day before the induction of FCA and thereafter, on day 4, 8, 12, 16, 20, 24, and day 28 using vernier calipers, and the percentage inhibition of the joint diameter was calculated.

Antinociceptive activity (Eddy's hot plate method). Antinociceptive activity was performed using Eddy's hot plate method,²¹ according to which the animal was placed on a hot plate and the instrument was started with a cut-off period of 18 seconds and 55 ± 0.1 °C maximum heat to avoid harming the animals; the reaction time (in seconds) was observed and the



time taken by the animal to start paw licking or jumping was noted.

Preparation of blood serum. For the preparation of blood serum, the blood sample was taken from rats by performing cardiac puncture. After cardiac puncture, blood was immediately collected in the serum gel separating tubes. Then, the test tubes were placed in the refrigerator at 4 °C for 15–20 minutes. Centrifugation was done at 3000 rpm for 20 minutes. The clear serum collected after centrifugation was transferred to Eppendorf tubes and refrigerated at –80 °C until needed.

Determination of hematological parameters. On the 28th day, blood was withdrawn from the rats by cardiac puncture. The hematological parameters were analyzed, including red blood cells (RBCs) count, hemoglobin (Hb), white blood cells (WBCs) count, platelet count (PLT), and erythrocyte sedimentation rate (ESR) using an automated hematological analyzer with a specific software for rat blood samples.

Biochemical estimation. On the 28th day, blood was withdrawn from the rats by cardiac puncture and the serum was separated and analyzed for the estimation of the biochemical parameters, including serum ALT (alanine aminotransferase), ALP (alkaline phosphatase), and AST (aspartate aminotransferase) using diagnostic kits provide by the Crescent Diagnostics Company.

TNF- α estimation. After the completion of the study, the rats were sacrificed, and their paws were separated. The TNF- α level in the paw tissue was determined by the commercially available ELISA kit from Glory Science Co., Ltd and the results were expressed in ng mL⁻¹.

Antioxidant activity

GSH analysis in the liver tissue. The estimation of the GSH content in the liver was assessed using the method of Sedlak and Lindsay²² with some little alterations. The liver tissue was homogenized in 67 mM phosphate buffer (pH 7.4). To homogenate, 25% of TCA was added to precipitate it. Then, the centrifugation of the homogenate was done at 4200 rpm at 4 °C for 40 minutes. Three replicates were made, each containing 200 mM Tris-HCl buffer containing 0.2 M EDTA of pH 7.4, the supernatant, 10 mM DTNB, and methanol. The mixture was vortexed and then kept for incubation at 37 °C for 30 minutes. At a wavelength of 412 nm, the absorbance was recorded using a UV-Vis spectrophotometer.

MDA analysis in the liver tissue. Estimation of MDA in the liver tissue was carried out using thiobarbituric (TBA) assay, followed by the method of Ohkawa²³ with some modifications. The liver samples were thawed and homogenized in 1.15% KCl solution to make 10% of the tissue homogenate. Three replicates were made, each containing 8% sodium lauryl sulfate, 20% acetic acid, 0.8% thiobarbituric acid, and distilled water, in which the tissue homogenate was added. The mixture was vortexed and centrifuged at 4000 rpm for 30 minutes. At a wavelength of 532 nm, the absorbance of the supernatant was recorded using a UV-Vis spectrophotometer.

Catalase analysis in liver tissue. The estimation of the catalase activity was done using the method of Sinha²⁴ with some

little changes. The thawed liver samples were homogenized in 67 mM phosphate buffer (pH 7.4) to get 10% homogenate. Three replicates were made, each containing 0.2 M of hydrogen peroxide, 0.01 M of phosphate buffer (pH 7.0), and 10% tissue homogenate to make the final volume upto 3 mL. In a boiling water bath, all the test tubes were heated for 10 minutes. At a wavelength of 570 nm, the absorbance was recorded using a UV-Vis spectrophotometer.

Superoxide dismutase analysis in the liver tissue. The estimation of the superoxide dismutase activity was carried out by the method of Magnani²⁵ with some slight alterations. The thawed liver samples were homogenized in 67 mM phosphate buffer (pH 7.4). Three replicates were made, each containing Tris-HCl and homogenate. Then, 0.2 mM pyrogallol solution was added to both the control and the sample test tubes. Blank test tubes contained only Tris-EDTA buffer (pH 8.2). At a wavelength of 532 nm, the absorbance was recorded using a UV-Vis spectrophotometer. The absorbance of the control and the sample test tubes was recorded at 0 and 1 min immediately after the addition of the pyrogallol solution. The estimation of the superoxide dismutase activity was carried out by the following formula.

$$\text{SOD activity (U mL}^{-1}\text{)} = \frac{\% \text{ inhibition of pyrogallol autoxidation}}{50\%}$$

X-ray radiographic assessment

On the 28th day, radiographs were taken for the hind paw of all the experimental animals using an X-ray unit. Radiographs were examined for soft tissue swelling, narrowing of the spaces between the joints, osteolysis, and bony erosions.

Statistical analysis

For the statistical analysis of the results, Graph pad prism version 7.01 was used. Analysis was done using an unpaired *t*-test and one-way ANOVA, followed by post hoc Dunette's test for comparison among different groups. All the data were expressed in mean \pm standard deviation (mean \pm SD) and *p* < 0.05 was considered as statistically significant.

Results and discussion

UV/Vis analysis of the synthesized AuNPs

The aqueous extract of *Manilkara zapota* was added into a flask containing gold solution. The formation of AuNPs was confirmed by the development of a purple color, which is a characteristic of the AuNPs. The color change from light yellow to purple is due to the excitation of surface plasmon resonance (SPR) in the AuNPs induced by passing light and this observation was confirmed by UV-Vis spectral analysis. The change in the SPR of the AuNPs with respect to the reaction time can be seen in Fig. 1. The intensity of the color as well as the absorbance values increased gradually in the reaction medium along with the reaction time, which implied an increasing AuNPs concentration and the continuous reduction of gold



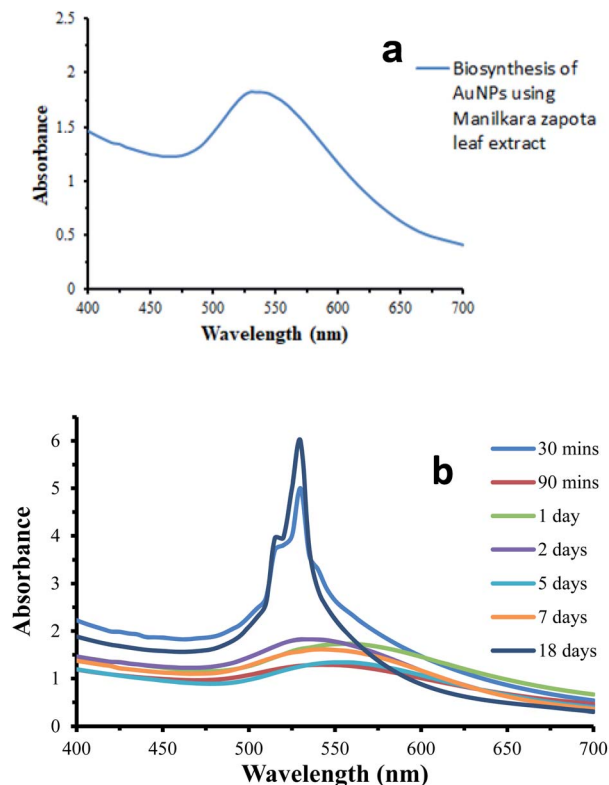


Fig. 1 (a) UV/Vis spectrum of biosynthesized AuNPs, (b) Stability of the biosynthesized AuNPs.

ions. AuNPs from the *Manilkara zapota* leaf extract (Fig. 1b) showed a weak SPR band at 530 nm and after 90 min, a red shift was observed in SPR at 545 nm due to a slight modification in the size and shape of the AuNPs. This red shift is attributed to the aggregation and clustering of gold nanoparticles and thus an increase in the size of the nanoparticles and the shift in the SPR band was observed.^{26–28} A gradual increase in the absorption intensity and saturation at an absorbance value of 5.999 indicate the complete reduction of gold ions in the reaction medium (Fig. 2). The incubation period of 18 days did not show

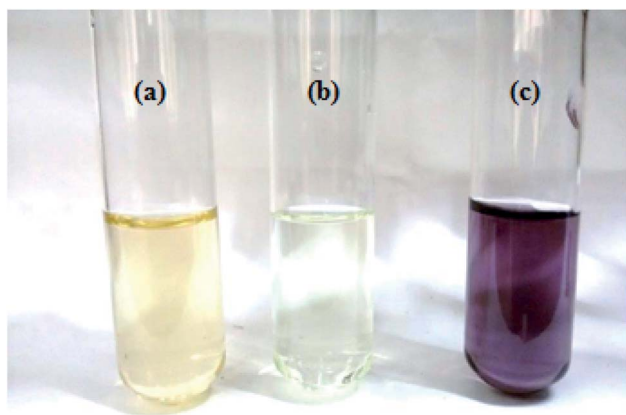


Fig. 2 (a) Aqueous extract of leaves, (b) $\text{HAuCl}_4 \cdot 3\text{H}_2\text{O}$ solution, (c) AuNPs solution.

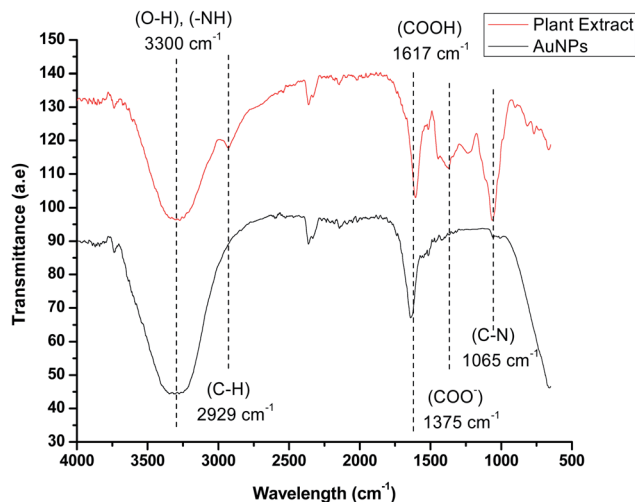


Fig. 3 FTIR spectrum of the plant extract and the AuNPs.

any considerable change in the SPR intensity of *Manilkara zapota*, thereby ascertaining the stability of the biosynthesized AuNPs. In Fig. 1b, the absorbance of about 530–560 nm is due to the SPR exhibited by spherical nanoparticles. The biosynthesized AuNPs show a relatively sharper absorbance peak at about 530 nm in Fig. 1a. The stability of the AuNPs biosynthesized at room temperature in neutral pH in the absence of the salt with 1 mM concentration of aqueous gold chloride solution was studied over a period of 18 days. The biosynthesized AuNPs were stable enough till 20 days (Fig. 1b).

FTIR analysis of the synthesized AuNPs

FTIR analysis was performed to determine the presence of various phytochemical constituents in the extract of *Manilkara zapota*, which is responsible for the reduction and stabilization of AuNPs by capping their surface. The FTIR spectra show a peak at 3300–3600 cm^{-1} due to the stretching vibrations of the polyphenolic O–H group and primary amine N–H. These peaks indicated the presence of alkaloids, terpenoids, flavonoids, and coumarins, which are responsible for the stabilization of the AuNPs. The FTIR spectra show a peak at 2929 cm^{-1} due to the

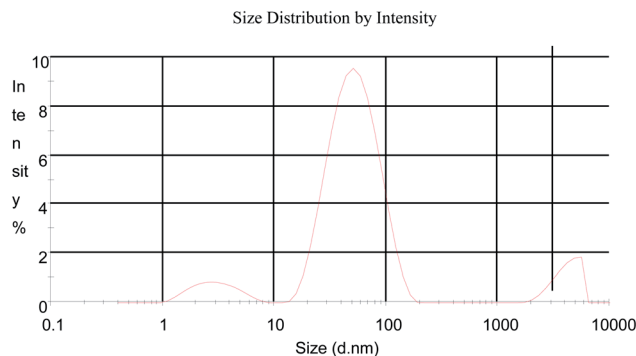


Fig. 4 Size distribution of the AuNPs synthesized from the *Manilkara zapota* leaf extract.



C–H stretching vibrations of the alkane group. The presence of the carboxyl group on the surface was confirmed by the presence of a strong band at 1617 cm^{-1} . A weak band at 1375 cm^{-1} indicated the asymmetric stretching of the carboxylate ion. The band at 1243 cm^{-1} indicated the presence of C–O stretching of the carboxylic acid group. The strong band observed at 1065 cm^{-1} indicates the presence of the C–N stretching

vibration of the aliphatic amines. The IR spectra of AuNPs in the figure showed weaker bands at about 2929 and 1065 cm^{-1} , and suppressed bands at 1375 and 1243 cm^{-1} compared with the extract (Fig. 3). This observation revealed that the plant extract having amine and hydroxyl functional groups could possibly be associated to the reduction as well as the stabilization of the AuNPs.

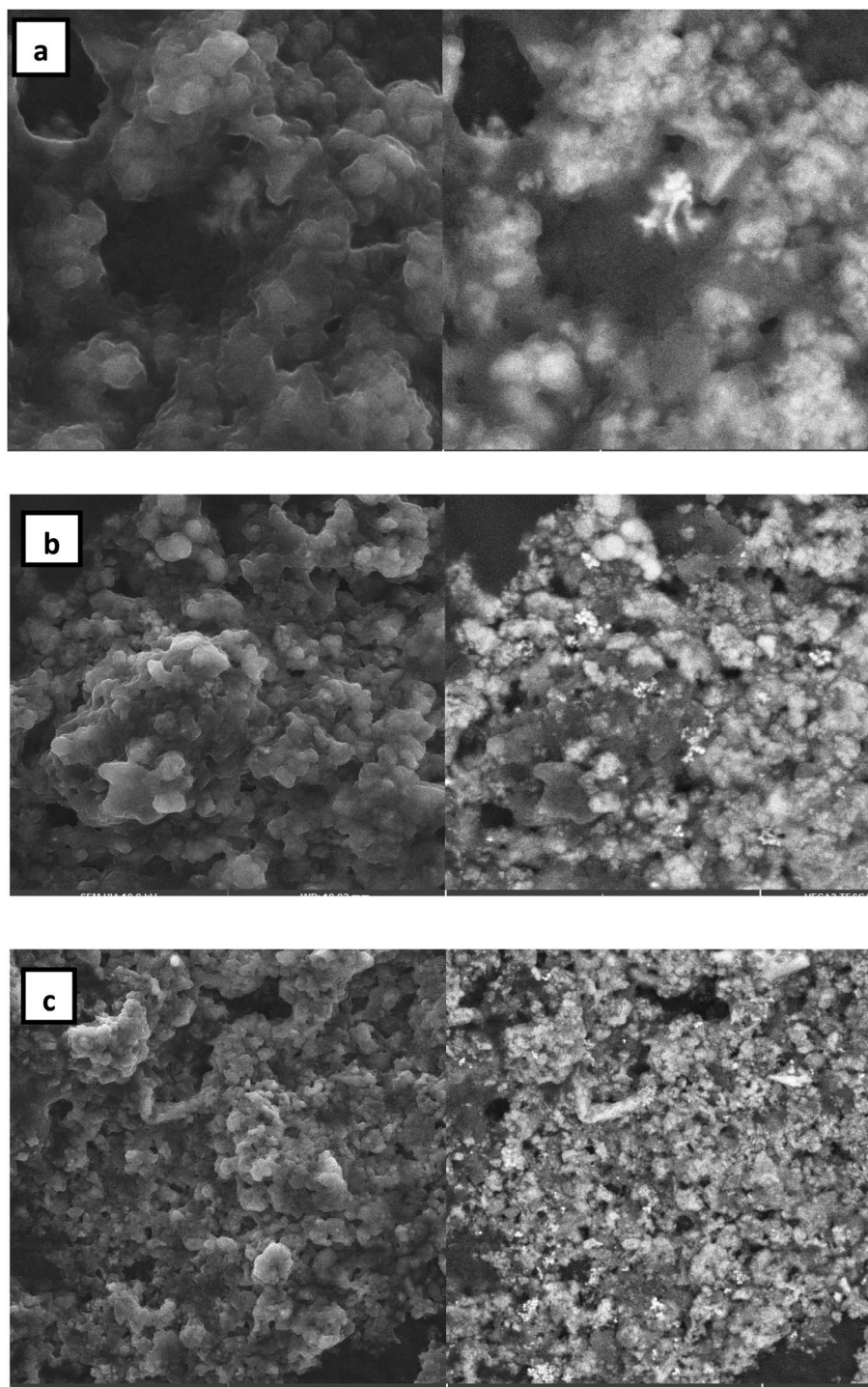


Fig. 5 SEM images of the AuNPs formed by the reaction of 1 mM H AuCl_4 and 1% *Manilkara zapota* leaf extract at 25°C reaction temperature. (a) $2\ \mu\text{m}$, (b) $10\ \mu\text{m}$, and (c) $20\ \mu\text{m}$.



Dynamic light scattering (DLS) and zeta potential studies

DLS has been used to measure the particle sizes in the colloidal solution and the size distribution data of the AuNPs obtained at pH 7 from *Manilkara zapota* is shown in Fig. 4. The average particle size distribution is 41.90 ± 27.42 (Z average \pm (SD) d nm) for AuNPs synthesized from *Manilkara zapota* leaf extract with a polydispersity index of 0.477. The zeta potential and zeta deviation values obtained are -20.8 and 48.8 mV, respectively. The zeta potential values obtained imply a stable dispersion of the biosynthesized AuNPs. A zeta potential higher than 30 mV or lesser than -30 mV is indicative of a stable system. The large negative potential value suggests the presence of negatively charged moieties in the extracts that confer electrostatic stability to the nanoparticles.

Scanning electron microscopy (SEM) analysis

The AuNPs were subjected to SEM imaging to ascertain the morphological features. The low magnification image (Fig. 5a) shows the formation of spherical nanoparticles of size in the range of 40 – 200 nm. At higher magnification (Fig. 5b), spherical AuNPs were clearly observed. SEM reveals that each spherical particle is made up of an aggregate of even smaller nanoparticles.

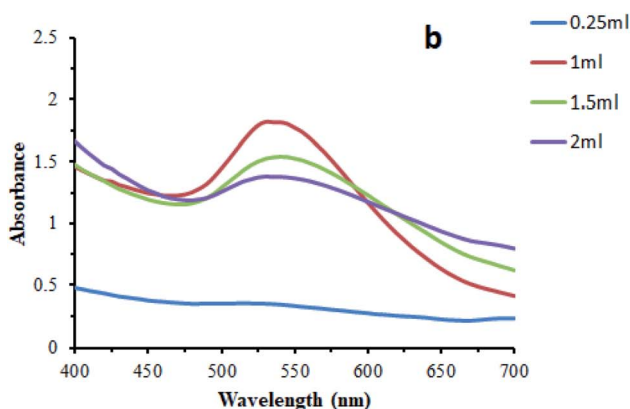
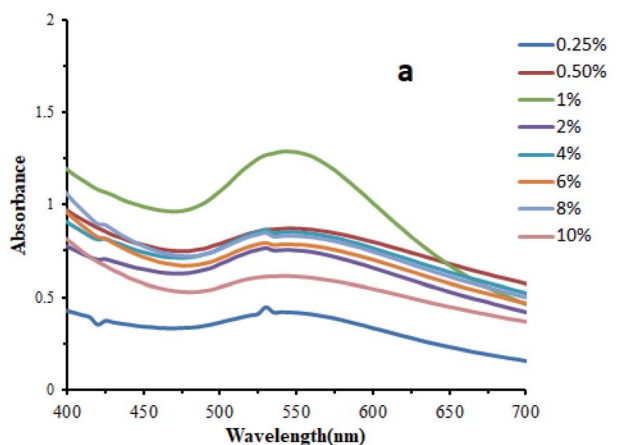


Fig. 6 Effect of concentration of the leaf extract on the biosynthesis of the AuNPs. (a) change in the concentration of the leaf extract, (b) change in the volume of the leaf extract (1%).

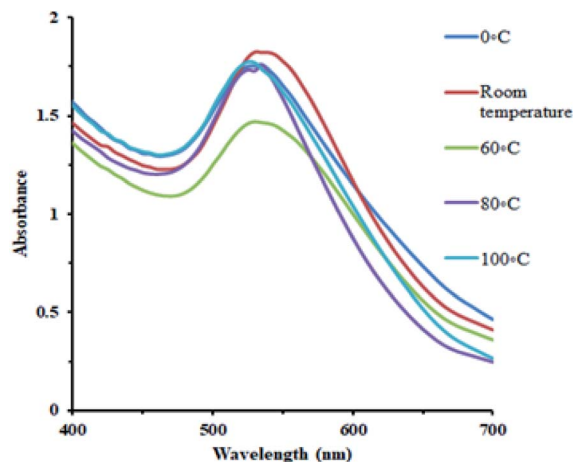


Fig. 7 Effect of temperature on AuNPs synthesis.

Effect of concentration of the leaf extract

The biosynthesis of AuNPs was carried out with changing concentration of the leaf extract. It was observed that the alteration in the concentration of the leaves extract has a slight effect on the formation and stability of the AuNPs. 1 mL leaf extract of a wide range of varying concentrations including 0.25 , 0.5 , 1 , 2 , 4 , 6 , 8 , and 10% with 6 mL of 1 mM gold chloride solution at room temperature and neutral pH were employed. The optimum concentration for the biosynthesis of AuNPs was 1% . Biosynthesis with this concentration showed maximum absorbance. The effect of concentration of the leaf extract was also studied using varying concentrations of 1% leaf extract as 0.25 mL, 1 mL, 1.5 mL, and 2 mL. The optimum concentration was found to be 1 mL for the biosynthesis of AuNPs (Fig. 6).

Effect of temperature

AuNPs were synthesized under a wide range of temperature conditions. The effect of temperature on the conversion of gold ions to metallic gold is shown in the figure. A wide range of

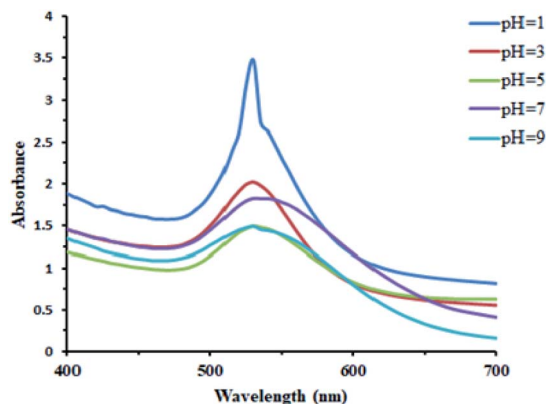


Fig. 8 Effect of the change in the pH on the biosynthesis of AuNPs.



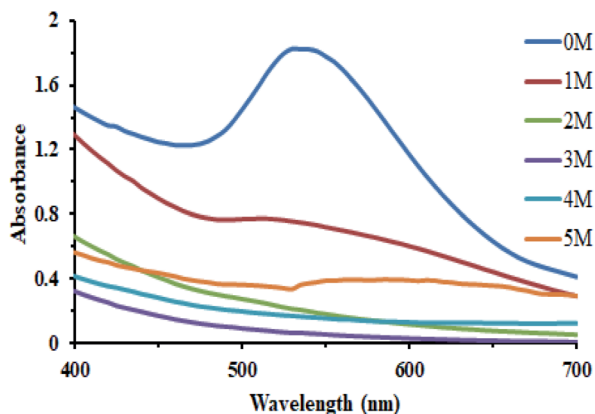


Fig. 9 Effect of the salt concentration on the biosynthesis of AuNPs.

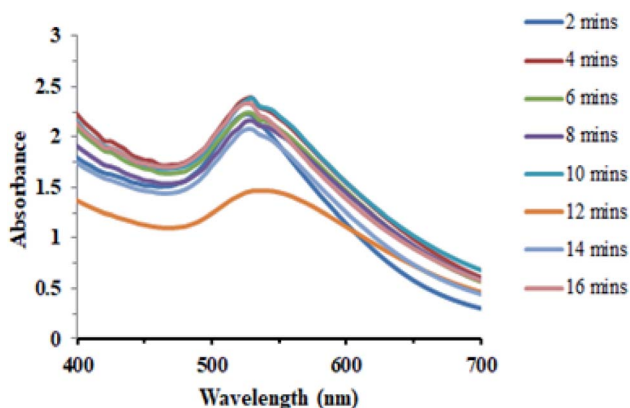


Fig. 10 Effect of the reaction time on the biosynthesis of AuNPs.

temperature was employed including 0 °C, room temperature, 60, 80, and 100 °C at neutral pH. The UV spectra indicated that there is high amount of antioxidants in the plant extract so that the change in the color and absorbance at 530 nm is designated even at 0 °C. The optimum condition for the conversion of gold

ions into AuNPs was observed at room temperature. The stability of the synthesized AuNPs at room temperature was also significant (Fig. 7).

Effect of pH

AuNPs were synthesized under a wide range of pH conditions. The biosynthesis of AuNPs was carried out under a pH values of 1, 3, 5, 7, and 9. Basic conditions were not very favorable for their formation. Acidic and neutral conditions were favorable to some extent. The UV/Vis spectral study demonstrated that the acidic conditions are found to be the best for the AuNPs' formation (Fig. 8).

Effect of salt concentration

In order to study the effect of the salt on the stability of the biosynthesized AuNPs, an equal amount of the AuNPs reaction mixture was treated with varying concentrations of the NaCl solution including 1, 2, 3, 4, and 5 M. The presence of the salt had a marked effect on their stability, although the varying concentrations of the salt had almost the same outcome on the stability of the AuNPs (Fig. 9).

Effect of the reaction time

Another important factor that affected the synthesis of AuNPs was the reaction time. The synthesis of AuNPs was investigated since the start of reaction through a UV-Vis spectrophotometer. The progress in the reaction that was carried out at room temperature and neutral pH was monitored from time to time (Fig. 10).

Results of animal studies

In carrageenan-induced paw edema, the results showed that the paw volume in the diclofenac sodium, aqueous extract, and nanoparticles of *M. zapota* leaf extract treated groups significantly ($*p < 0.05$) decreased as compared to the carrageenan-induced control group. Nanoparticles of *M. zapota* leaf extract

Table 1 *In vivo* acute antiinflammatory activity of the aqueous extract and nanoparticles of the *M. zapota* leaf extract^a

Paw volume (mL) (% inhibition)

Groups	0 hour	1 st hour	2 nd hour	3 rd hour	4 th hour	5 th hour	6 th hour
Control	2.28 ± 0.14	3.18 ± 0.09	3.24 ± 0.12	3.28 ± 0.10	3.35 ± 0.11	3.29 ± 0.08	3.19 ± 0.05
Positive control	2.32 ± 0.08	2.71 ± 0.10*	2.64 ± 0.11*	2.57 ± 0.14*	2.53 ± 0.13*	2.51 ± 0.14*	2.44 ± 0.13*
		(56.67)	(66.67)	(75.0)	(80.37)	(81.18)	(86.81)
AEMZ (200 mg kg ⁻¹)	2.26 ± 0.20	2.85 ± 0.09*	2.87 ± 0.11*	2.79 ± 0.10*	2.74 ± 0.11*	2.70 ± 0.11*	2.64 ± 0.11*
		(34.44)	(36.45)	(47.0)	(55.14)	(56.43)	(58.24)
AEMZ (400 mg kg ⁻¹)	2.11 ± 0.23	2.66 ± 0.15*	2.68 ± 0.16*	2.60 ± 0.13*	2.54 ± 0.11*	2.50 ± 0.09*	2.42 ± 0.09*
		(38.89)	(40.68)	(51.0)	(59.81)	(61.38)	(65.93)
NPMZ (4 mg kg ⁻¹)	2.27 ± 0.16	2.78 ± 0.18*	2.80 ± 0.18*	2.72 ± 0.19*	2.66 ± 0.20*	2.60 ± 0.18*	2.55 ± 0.18*
		(43.33)	(44.79)	(55.0)	(63.55)	(67.32)	(69.23)
Gold NPMZ (5 mg kg ⁻¹)	2.15 ± 0.28	2.62 ± 0.14*	2.60 ± 0.14*	2.56 ± 0.13*	2.50 ± 0.13*	2.45 ± 0.12*	2.39 ± 0.12*
		(46.67)	(53.12)	(59.0)	(67.28)	0.12*(70.29)	(73.62)

^a Comparison among the carrageenan control group and all other groups was conducted using one way ANOVA, followed by Dunette's test. Values are expressed as mean ± SD ($n = 4$). $*p < 0.05$ represents a significant decrease in the paw volume as compared to the control group.





Table 2 Effect of the aqueous extract and nanoparticles of *M. zapota* leaf extract on the paw volume (mL) in FCA-induced arthritic rats^a

Groups	Paw volume (mL) (% inhibition)									
	Day 0	Day 4	Day 8	Day 12	Day 16	Day 20	Day 24	Day 28		
Normal control	2.29 ± 0.13	2.30 ± 0.15	2.31 ± 0.14	2.31 ± 0.13	2.32 ± 0.13	2.33 ± 0.16	2.34 ± 0.18	2.34 ± 0.10		
Arthritic control	2.32 ± 0.12	4.32 ± 0.06 ^{ab}	4.19 ± 0.11 ^{ab}	4.42 ± 0.03 ^{ab}	4.49 ± 0.11 ^{ab}	4.54 ± 0.13 ^{ab}	4.49 ± 0.13 ^{ab}	4.42 ± 0.11 ^{ab}		
Positive control	2.25 ± 0.08	4.26 ± 0.09	4.15 ± 0.09	4.37 ± 0.07	3.82 ± 0.13 [*] (27.64)	3.51 ± 0.09 [*] (43.24)	3.04 ± 0.09 [*] (63.59)	2.57 ± 0.13 [*] (84.76)		
AEMZ (200 mg kg ⁻¹)	2.31 ± 0.08	4.23 ± 0.14	4.12 ± 0.12	4.34 ± 0.11	4.22 ± 0.14 [*] (11.98)	3.99 ± 0.12 [*] (24.32)	3.56 ± 0.17 [*] (42.39)	3.12 ± 0.12 [*] (61.42)		
AEMZ (400 mg kg ⁻¹)	2.33 ± 0.06	4.27 ± 0.08	4.19 ± 0.09	4.37 ± 0.06	4.17 ± 0.09 [*] (15.2)	3.89 ± 0.14 [*] (29.72)	3.44 ± 0.15 [*] (48.84)	3.01 ± 0.28 [*] (67.61)		
Gold NPMZ (5 mg kg ⁻¹)	2.16 ± 0.24	4.27 ± 0.13	4.15 ± 0.12	4.34 ± 0.12	3.92 ± 0.16 [*] (18.89)	3.64 ± 0.07 [*] (33.33)	3.11 ± 0.08 [*] (56.22)	2.76 ± 0.08 [*] (71.42)		

^a Statistical analysis of the results was conducted between the arthritic group and the control group using the unpaired *t*-test. Comparison among the arthritic group and all the other groups was conducted using one way ANOVA, followed by Dunette's test. Values are expressed as mean ± SD (*n* = 4). (^{ab}*p* < 0.05) represents significance.

showed a more prominent effect on the % inhibition of the paw edema as compared to the aqueous extract (Table 1).

In FCA-induced arthritis, the paw volume and joint diameter is significantly (*p* < 0.05) decreased in the indomethacin, aqueous extract, and nanoparticles of *M. zapota* treated groups as compared to the FCA-induced arthritic group, as shown in Tables 2 and 3. A significant decrease in the paw volume and joint diameter was observed from 16 to 28 days. The effect of the aqueous extract and the nanoparticles of *M. zapota* leaves at the latency time (seconds) in FCA-induced arthritic rats is presented in Table 4 and showed a marked improvement.

In the present study, hematological analysis revealed that the hemoglobin content and RBCs count significantly (*p* < 0.05) increased in indomethacin, aqueous extract, and gold nanoparticles of the *M. zapota* leaf extract treated groups as compared to the FCA-induced arthritic group, as shown in Table 5. Furthermore ESR, WBC's count, and platelet count significantly (*p* < 0.05) decreased in indomethacin, aqueous extract, and gold nanoparticles of the *M. zapota* leaf extract treated groups as compared to the FCA-induced arthritic group.

In the biochemical analysis, the results showed that the aqueous extract of *M. zapota* significantly (*p* < 0.05) decreased the ALT activity (28.53%) and (39.33%), the AST activity (29.09%) and (33.51%), the ALP activity (31.91%) and (32.56%), respectively, at doses of 200 and 400 mg kg⁻¹. Gold nanoparticles decreased the ALT activity (44.13%), AST activity (37.85%), and ALP activity (34.41%) compared to the FCA-induced arthritic group, as shown in Table 6.

The sub-acute antiarthritic activity results showed that the level of TNF- α in the paws of the arthritic control group is significantly increased as compared to the control group (Table 7).

In the antioxidant analysis, the results showed that the aqueous extract of *M. zapota* significantly (*p* < 0.05) increased the tGSH content (58.34%) and (68.91%), CAT activity (54.97%) and (72.05%), SOD activity (36.72%) and (51.48%), respectively, at doses of 200 and 400 mg kg⁻¹. Biosynthesized gold nanoparticles increased the tGSH content (75.74%), CAT activity (78.43%), and SOD activity (71.99%) as compared to the FCA-induced arthritic group, as shown in Table 8.

Radiological examination of X-rays in FCA-induced arthritic group showed a marked increase in the inflammation along with the inflammatory cells and the area of soft tissues is transparent or less dark as compared to the control group tissues (Fig. 11 and 12). This is due to the inflammatory process occurring at the joint level. While indomethacin, aqueous extract, and nanoparticles of *M. zapota* leaf extract showed a marked decrease in the inflammation along with the inflammatory cells and the area of the soft tissues becomes darker or less transparent as compared to the FCA-induced arthritic group (Fig. 13–16).

In carrageenan-induced paw edema, the results showed that the paw volume in the diclofenac sodium, aqueous extract, and nanoparticles of *M. zapota* leaf extract treated groups significantly (*p* < 0.05) decreased as compared to the carrageenan-induced control group. Nanoparticles of *M. zapota* showed

Table 3 Effect of the aqueous extract and nanoparticles of *M. zapota* on the joint diameter (mm) in FCA-induced arthritic rats^a

Joint Diameter (mm) (% inhibition)								
Groups	Day 0	Day 4	Day 8	Day 12	Day 16	Day 20	Day 24	Day 28
Normal control	4.25 ± 0.08	4.26 ± 0.08	4.27 ± 0.09	4.26 ± 0.08	4.27 ± 0.06	4.28 ± 0.08	4.28 ± 0.07	4.29 ± 0.09
Arthritic control	4.51 ± 0.06	7.10 ± 0.16 ^{**a}	6.91 ± 0.80 ^{**a}	7.44 ± 0.44 ^{**a}	7.74 ± 0.81 ^{**a}	8.09 ± 0.33 ^{**a}	7.77 ± 0.50 ^{**a}	7.33 ± 0.30 ^{**a}
Positive control	4.26 ± 0.13	7.09 ± 0.05	6.84 ± 0.19	7.13 ± 0.11	6.43 ± 0.16*	5.92 ± 0.25*	5.31 ± 0.14*	4.73 ± 0.35*
AEMZ (200 mg kg ⁻¹)	4.42 ± 0.12	7.02 ± 0.11	6.87 ± 0.21	7.12 ± 0.12	7.03 ± 0.21*	6.84 ± 0.18*	6.34 ± 0.17*	5.82 ± 0.33*
AEMZ (400 mg kg ⁻¹)	4.38 ± 0.08	7.05 ± 0.16	6.81 ± 0.13	7.04 ± 0.19	6.94 ± 0.17*	6.65 ± 0.12*	6.17 ± 0.13*	5.48 ± 0.35*
NPMZ (5 mg kg ⁻¹)	4.34 ± 0.06	6.91 ± 0.22	6.82 ± 0.16	7.17 ± 0.21	6.68 ± 0.15*	6.48 ± 0.11*	5.79 ± 0.16*	5.18 ± 0.20*

^a Statistical analysis of results was conducted between the arthritic group and the control group using the unpaired *t*-test. Comparison among the arthritic group and all other groups was conducted using one way ANOVA, followed by Dunette's test. Values are expressed as mean ± SD (*n* = 4). (^{**a}*p* < 0.05) represents significance.

Table 4 Effect of the aqueous extract and nanoparticles of *M. zapota* leaves on the latency time (seconds) in FCA-induced arthritic rats^a

Latency time (secs)								
Groups	Day 0	Day 4	Day 8	Day 12	Day 16	Day 20	Day 24	Day 28
Normal control	8.5 ± 1.29	8.9 ± 0.85	8.5 ± 1.29	8.3 ± 0.96	8.8 ± 0.96	8.62 ± 1.15	8.8 ± 0.96	9.0 ± 0.81
Arthritic control	8.9 ± 0.95	7.6 ± 1.25	7.2 ± 0.56	6.4 ± 0.48 ^{**a}	6.2 ± 0.76 ^{**a}	6.0 ± 0.78 ^{**a}	5.0 ± 1.63 ^{**a}	4.5 ± 1.29 ^{**a}
Positive control	8.6 ± 0.95	8.3 ± 0.96	7.5 ± 1.29	6.3 ± 0.96	12.3 ± 0.96*	14.5 ± 1.29*	17.0 ± 1.83*	20.3 ± 2.22*
AEMZ (200 mg kg ⁻¹)	8.0 ± 0.82	7.3 ± 0.96	6.4 ± 0.85	5.7 ± 0.57	8.05 ± 1.02	9.9 ± 0.85*	11.6 ± 0.94*	13.0 ± 0.91*
AEMZ (400 mg kg ⁻¹)	8.0 ± 0.82	7.3 ± 1.71	6.5 ± 6.50	5.3 ± 0.96	7.88 ± 1.93	10.1 ± 1.65*	12.5 ± 1.29*	15.5 ± 1.29*
NPMZ (5 mg kg ⁻¹)	9.0 ± 0.69	7.5 ± 1.29	6.5 ± 1.29	5.9 ± 0.87	10.0 ± 0.82*	15.0 ± 1.83*	17.1 ± 2.09*	17.3 ± 2.22*

^a Statistical analysis of results was conducted between the arthritic group and the control group using the unpaired *t*-test. Comparison among the arthritic group and all other groups was conducted using one way ANOVA, followed by Dunette's test. Values are expressed in mean ± SD (*n* = 4). (^{**a}*p* < 0.05) represents significance.

a more prominent effect on the % inhibition of paw edema as compared to the aqueous extract.

Discussion

Arthritis induced by Freund's Complete Adjuvant (FCA) is primary and secondary chronic arthritis. In the primary

inflammatory phase, the generation of prostaglandins occurs and the secondary is an immunological state in which autoantibodies are generated. FCA is responsible for the stimulation of cell mediated immunity and ultimately increases the production of immunoglobulins (20). TNF- α is an important cytokine that is associated with joint inflammation and destruction through chemokine expression, activation of cytokine,

Table 5 Sub-acute effect of the aqueous extract and nanoparticles of *M. zapota* leaf extract on the hematological parameters in FCA-induced arthritic rats^a

Groups	ESR (mm/1st an Hour)	Hemoglobin content (g dL ⁻¹)	RBC's count (10 ⁶ μ L ⁻¹)	WBC's count (1000 μ L ⁻¹)	Platelet count (1000 μ L ⁻¹)
Normal control	2.50 ± 1.00	13.68 ± 0.34	7.53 ± 0.41	7.55 ± 3.15	584.3 ± 35.14
Arthritic control	10.50 ± 2.52 ^{**a}	10.28 ± 0.51 ^{**a}	4.55 ± 0.70 ^{**a}	18.85 ± 1.57 ^{**a}	848 ± 49.71 ^{**a}
Positive control	3.00 ± 1.16*	13.50 ± 0.26*	7.28 ± 0.34*	8.15 ± 0.59*	555.8 ± 28.66*
AEMZ (200 mg kg ⁻¹)	5.00 ± 1.16*	12.28 ± 0.45*	6.50 ± 0.45*	9.73 ± 0.84*	685.8 ± 120.2*
AEMZ (400 mg kg ⁻¹)	4.50 ± 1.00*	12.43 ± 0.15*	6.80 ± 0.57*	9.23 ± 0.54*	604.5 ± 57.05*
NPMZ (5 mg kg ⁻¹)	4.00 ± 1.63*	12.65 ± 0.26*	7.08 ± 0.28*	8.80 ± 0.55*	652.8 ± 92.69*

^a Statistical Analysis of the results was conducted between the arthritic group and the control group using the unpaired *t*-test. Comparison among the arthritic group and all other groups was conducted using one way ANOVA, followed by Dunette's test. Values are expressed in mean ± SD (*n* = 4). (^{**a}*p* < 0.05) represents significance.



Table 6 Sub-acute effect of the aqueous extract and nanoparticles of *M. zapota* leaf extract on the biochemical parameters in FCA-induced arthritic rats^a

Groups	ALT activity (U L ⁻¹)	AST activity (U L ⁻¹)	ALP activity (U L ⁻¹)
Normal control	36.76 ± 5.78	44.67 ± 5.98	117.4 ± 6.69
Arthritic control	72.87 ± 5.24 ^{**a}	84.60 ± 3.14 ^{**a}	220.6 ± 34.79 ^{**a}
Indomethacin(4 mg kg ⁻¹)	40.72 ± 5.18*	47.70 ± 3.54*	130.0 ± 4.931*
AEMZ (200 mg kg ⁻¹)	52.08 ± 2.03*	60.00 ± 5.66*	148.5 ± 7.18*
AEMZ (400 mg kg ⁻¹)	48.41 ± 11.37*	56.26 ± 4.11*	151.5 ± 8.93*
Gold NPMZ (5 mg kg ⁻¹)	40.72 ± 3.42*	52.59 ± 3.46*	142.5 ± 5.82*

^a Statistical analysis of the results was conducted between the arthritic group and the control group using the unpaired *t*-test. Comparison among the arthritic group and all the other groups was conducted using one way ANOVA, followed by Dunette's test. Values are expressed in mean ± SD (*n* = 4). (^{**a}*p* < 0.05) represents significance.

Table 7 Sub-acute effect of the aqueous extract and nanoparticles of *M. zapota* leaf extract on the TNF- α level in FCA-induced arthritic rats^a

Groups	TNF- α level (ng mL ⁻¹)
	Mean ± SD
Normal control	24.12 ± 2.51
Arthritic control	60.05 ± 1.15 ^{**a}
Positive control	28.43 ± 0.47*
AEMZ (200 mg kg ⁻¹)	45.28 ± 1.95*
AEMZ (400 mg kg ⁻¹)	35.56 ± 2.36*
NPMZ (5 mg kg ⁻¹)	29.33 ± 0.64*

^a Statistical analysis of results was conducted between the arthritic group and the control group using the unpaired *t*-test. Comparison among the arthritic group and all other groups was conducted using one way ANOVA, followed by Dunette's test. Values are expressed in mean ± SD (*n* = 4). (^{**a}*p* < 0.05) represents significance.

protection of synovial fibroblasts, expression of endothelial-cell adhesion molecules, promotion of angiogenesis, suppression of regulatory T-cells, and induction of pain.²⁶ The blocking of TNF- α with monoclonal antibodies and the hindering of a soluble TNF-receptor fusion protein result in the prevention of arthritis.²⁹

In rheumatoid arthritis, the administration of gold compounds results in the accumulation of gold in the lysosomes of synovial macrophages. In the synovial lining, gold

compounds inhibit IL-1, IL-6, and TNF- α production, significantly decreasing the macrophage numbers and oxygen radical generation. Gold salts also inhibit angiogenic properties of the macrophages and inhibit T-cell proliferation in response to antigen or mitogen.³⁰ *Manilkara zapota* was tested for *in vitro* antiarthritic activity using inhibition of the protein denaturation model. *M. zapota* showed significant protection against the denaturation of proteins, which showed that it could be used as an antiarthritic.³¹ Keeping this in mind, it was hypothesized that gold nanoparticles of the *Manilkara zapota* leaf extract would prove beneficial against arthritis.

In the present study, gold nanoparticles of *M. zapota* leaf extract showed more prominent decrease in the paw volume and joint diameter as compared to the aqueous extract. The presence of terpenoids, tannins, flavonoids, and steroids may contribute to antiarthritic activity of *M. zapota* in reducing the paw volume and joint diameter.¹⁰ Plant-based nanoparticles offers advantages such as use of safer solvents, decreased use of dangerous reagents, feasibility, as well as their adaptability in use for pharmaceutical, surgical, and medicinal applications.³² Gold nanoparticles (AuNPs) are a promising class of nanomaterials that are inert in the biological environment. They have physical properties that are suitable in various biomedical applications owing to their unique size and shape. These include high surface, special optoelectronic properties, biocompatibility, charge-to-size ratio, and a tunable surface, which make them ideal for drug delivery, bio-sensing, and

Table 8 Sub-acute effect of the aqueous extract and nanoparticles of *M. zapota* leaf extract on the biomarkers in FCA-induced arthritic rats^a

Groups	tGSH content (mM g ⁻¹ tissue)	MDA level (μ M g ⁻¹ tissue)	Catalase activity (μ mol H ₂ O ₂ per mg per min)	SOD activity (U mg ⁻¹)
Normal control	4.28 ± 0.11	1.99 ± 0.29	43.89 ± 3.79	4.62 ± 0.42
Arthritic control	1.64 ± 0.23 ^{**a}	3.93 ± 0.33 ^{**a}	17.18 ± 3.09 ^{**a}	1.84 ± 0.19 ^{**a}
Positive control	3.17 ± 0.35*	2.31 ± 0.32*	32.36 ± 4.44*	3.55 ± 0.45*
AEMZ (200 mg kg ⁻¹)	2.59 ± 0.35*	3.09 ± 0.24*	26.63 ± 2.69*	2.51 ± 0.19*
AEMZ (400 mg kg ⁻¹)	2.76 ± 0.24*	2.91 ± 0.37*	29.56 ± 3.71*	2.78 ± 0.24*
Gold NPMZ (5 mg kg ⁻¹)	2.87 ± 0.29*	2.74 ± 0.28*	30.66 ± 3.94*	3.06 ± 0.12*

^a Statistical analysis of the results was conducted between the arthritic group and the control group using the unpaired *t*-test. Comparison among arthritic group and all other groups was conducted using one way ANOVA, followed by Dunette's test. Values are expressed in mean ± SD (*n* = 4). (^{**a}*p* < 0.05) represents significance.





Fig. 11 Radiograph of the left hind paw of the rat of the control group.



Fig. 12 Radiograph of the left hind paw of the rat of the FCA-induced arthritic group.



Fig. 13 Radiograph of the left hind paw of the rat of the indomethacin group.



Fig. 14 Radiograph of the left hind paw of the rat of the aqueous extract 200 mg kg⁻¹ group.





Fig. 15 Radiograph of the left hind paw of the rat of the aqueous extract 400 mg kg⁻¹ group.



Fig. 16 Radiograph of the left hind paw of the rat of the nanoparticles group.

diagnostic applications. Depending on the application, gold nanoparticles are prepared in different shapes, sizes, and structures.³³

In sub-acute antiarthritic activity, the aqueous extract has shown 61.42 and 67.61% inhibition of paw edema in volume at doses of 200 and 400 mg kg⁻¹, respectively, at the 28th day, as shown in Table 2. The biosynthesized gold nanoparticles showed 71.42% and indomethacin showed 84.76% inhibition of paw edema at the 28th day. The percentage inhibition of paw edema volume by aqueous and biosynthesized gold nanoparticles of *M. zapota* leaf extract could be attributed to some active constituents such as oleanic acid, myricitin-3-*O*- α -*L*-rhamnoside, and apigenin-7-*O*- α -*L*-rhamnoside present in the leaves of *M. zapota*.³⁴

In sub-acute antiarthritic activity, the aqueous extract showed 50.38 and 61.19% inhibition of paw edema in the joint diameter at doses of 200 and 400 mg kg⁻¹, respectively, at the 28th day. Nanoparticles exhibited 70.51% inhibition and indomethacin showed 83.34% inhibition of paw edema at the 28th day, as shown in Table 3. Nanoparticles of *M. zapota* leaf extract displayed a more prominent effect on the % inhibition of paw edema in the joint diameter as compared to the aqueous one. In rheumatoid arthritis, gold compounds cause a significant decrease in the macrophage numbers and inhibit T-cell proliferation in response to antigen or mitogen in the synovial lining.³⁵

Moreover, antinociceptive response with the aqueous extract and nanoparticles of *M. zapota* leaf extract-treated groups significantly ($*p < 0.05$) increased the latency time as compared to the FCA-induced arthritic group, as shown in Table 4. Nanoparticles of *M. zapota* leaf extract demonstrated a more prominent increase in the latency time as compared to the aqueous extract. The RBC count and hemoglobin levels were reported to be decreased under arthritic conditions, which is a common reason of anemia in arthritic patients. WBCs and platelet count have been reported to increase in rheumatoid arthritis, which is due to the stimulation of the immune system in invading antigens. Biosynthesized gold nanoparticles proved more effective in increasing the Hb content and RBCs count and in decreasing the WBC's and platelets count as compared to the aqueous extract.^{36,37}

The ALT, AST, and ALP activity in the serum is the tool to measure the antiarthritic activity of a particular drug. In the inflammatory process, ALT and AST play an important role in the formation of biologically-active chemical mediators such as bradykinins. Elevated levels of ALP have been reported in liver and bone, which leads to localized bone loss in the form of bone erosion and periarticular osteopenia. In biochemical analysis, it has been revealed that the nanoparticles of *M. zapota* leaf extract showed a prominent decrease in the ALT, AST, and ALP activities as compared to the aqueous extract.³⁸

It has been reported that pro-inflammatory cytokines, including TNF- α , play an important role in the pathophysiology



of rheumatoid arthritis and its level increases in the bone region of the knee joint.^{39,40} The aqueous extract and biosynthesized gold nanoparticles of *M. zapota* leaf extract treated groups significantly decreased the level of TNF- α as compared to the FCA-induced arthritic group, as shown in Table 7. Gold nanoparticles showed more efficacies in decreasing the level of TNF- α as compared to the aqueous extract. In rheumatoid arthritis, gold compounds inhibit IL-1, IL-6, and TNF- α production and a significant decrease in the macrophage in the synovial lining.³⁶

Oxidative stress has been reported in rheumatoid arthritis, which occur due to the overproduction of ROS, which is produced during cellular oxidative phosphorylation and by activated phagocytic cells during oxidative bursts.⁴ The overproduction of the oxidative stress markers such as MDA was noticed in adjuvant-induced arthritis. This is because during inflammatory disease, phagocytes accumulate in the joint region and increase the levels of hydroxyl radicals, hydrogen peroxide, and superoxide radicals.^{35,41} The tGSH, SOD, and catalase activities were found to be decrease under the arthritic conditions.⁴² The current study revealed that nanoparticles of *M. zapota* leaf extract showed a prominent increase in the tGSH content, CAT activity, and SOD activity as compared to the aqueous and methanol extracts. Aqueous extract and gold nanoparticles of *M. zapota* leaf extract significantly ($*p < 0.05$) decreased the MDA level as compared to the FCA-induced arthritic animals. Moreover, nanoparticles of *M. zapota* leaf extract showed a prominent decrease in the MDA level as compared to the aqueous extract. The antioxidant potential of *M. zapota* leaves is due to the presence of high content of flavonoids and phenols.⁶ Gold compounds are also responsible for a significant decrease in oxygen radical generation in rheumatoid arthritis.³⁵ On a radiological basis, the improvement in the inflammatory condition due to biosynthesized gold nanoparticles of the *M. zapota* leaf extract illustrated a more potent effect as compared to the aqueous extract.⁴³

Conclusion

A facile, inexpensive, ecofriendly, non-hazardous, and green approach for the synthesis of AuNPs was developed through the reduction of aqueous HAuCl₄ solution using "*Manilkara zapota* leaf extract" as the reducing and stabilizing agent. The leaf extract was used to reduce gold ions into metallic gold. The antioxidants present in "*Manilkara zapota* leaf extract" served the purpose of reduction and stabilization. Thus, an ecofriendly and non-toxic plant extract can be used as a systematic substitute to traditional chemicals. The stability of the AuNPs was increased using plant polyphenolic compounds. Different analytical techniques such as UV, FTIR, XRD, SEM, and zeta potential were used for the confirmation of the AuNPs. Different factors affecting the synthesis of AuNPs such as the effect of concentration, temperature, pH, reaction time, and salt were studied. *Manilkara zapota* and its gold nanoparticles were screened for their antiarthritic activity. It was concluded that the aqueous extract and the gold nanoparticles of *M. zapota* leaves possess significant *in vivo* analgesic, anti-inflammatory,

and antiarthritic activity in FCA-induced arthritis. Biosynthesized gold nanoparticles of the aqueous extract of *M. zapota* leaves possess more pronounced antiarthritic activity and TNF- α inhibition as compared to the aqueous extract and can be used as a potent antiarthritic agent. Advanced studies are needed to identify the active phytoconstituent(s) of *M. zapota* responsible for its antiarthritic activity and also to validate its safety and efficacy.

Conflicts of interest

There is no conflict of the interest among the authors.

Abbreviations

AuNPs	Gold nanoparticles
CDNB	1-Chloro-2,4-dinitrobenzene
FCA	Freund's complete adjuvant
SOD	Superoxide dismutase
CAT	Catalase
MDA	Malondialdehyde
tGSH	Total glutathione
NSAIDs	Nonsteroidal anti-inflammatory drugs
DMARDs	Disease-modifying antirheumatic drugs
GSH	Reduced glutathione
AP	Alkaline phosphatase
ALT	Alanine transaminase
AST	Aspartate transaminase
TMP	Tetramethylpropane
ELISA	Enzyme-linked immunosorbent assay
EDTA	Ethylenediaminetetraacetic acid
TNF- α	Tumor necrosis factor alpha
TCA	Trichloroacetic acid

Acknowledgements

This work was financially supported by the Higher Education Commission (HEC) Pakistan, under the NRPU Research Grant, project no. 8639/Punjab/NRPU/R&D/HEC/2017, and TDF Research Grant, project no. TDF03-294. All the authors would like to acknowledge School of Chemistry, University of the Punjab and Punjab University College of Pharmacy (PUCP), University of the Punjab Lahore, Pakistan for facilitating this research work.

References

- H.-U. Scherer, T. Häupl and G. R. Burmester, *J. Autoimmun.*, 2020, **110**, 102400.
- P.-A. Juge, J. S. Lee, J. Lau, L. Kawano-Dourado, J. R. Serrano, M. Sebastiani, G. Koduri, E. Matteson, K. Bonfiglioli and M. Sawamura, *Eur. Respir. J.*, 2021, 57.
- A. Kanwal, L. Abida, A. Sana and S. A. Ahlam, *GSC Biol. Pharm. Sci.*, 2018, **5**, 50–55.
- C. A. Hitchon and H. S. El-Gabalawy, *Arthritis Res. Ther.*, 2004, **6**, 1–14.



- 5 R. Nair and S. Chanda, *Indian J. Pharm. Sci.*, 2008, **70**, 390.
- 6 S. Chanda and K. Nagani, *J. Nat. Sci.*, 2010, **8**, 260–266.
- 7 J. Ma, X. D. Luo, P. Protiva, H. Yang, C. Ma, M. J. Basile, I. B. Weinstein and E. J. Kennelly, *J. Nat. Prod.*, 2003, **66**(7), 983–986.
- 8 M. A. Osman, M. A. Aziz, M. R. Habib and M. R. Karim, *Int. J. Drug Dev. Res.*, 2011, **3**, 185–190.
- 9 S. M. Barbalho, P. C. d. S. Bueno, D. S. Delazari, E. L. Guiguer, D. P. Coqueiro, A. C. Araújo, M. d. S. S. de Souza, F. M. Farinazzi-Machado, C. G. Mendes and M. Groppo, *J. Med. Food*, 2015, **18**, 385–391.
- 10 K. Konuku, K. C. Karri, V. K. Gopalakrishnan, Z. Hagos, H. Kebede, T. K. Naidu, P. P. Noyola, J. Palleti and G. Rao Duddukuri, *Int. J. Curr. Pharm. Res.*, 2017, **9**, 130–134.
- 11 H. Hossain, M. S. I. Howlader, S. K. Dey, A. Hira and A. Ahmed, *Int. J. Pharm. Sci. Rev. Res.*, 2012, **3**, 4791–4795.
- 12 M. Singh, P. Soni, N. Upmanyu and Y. Shivhare, *Asian J. Pharm. Tech.*, 2011, **1**, 123–124.
- 13 H. Daraee, A. Eatemadi, E. Abbasi, S. Fekri Aval, M. Kouhi and A. Akbarzadeh, *Artif. Cells, Nanomed., Biotechnol.*, 2016, **44**, 410–422.
- 14 M. Rai, A. Yadav and A. Gade, *Crit. Rev. Biotechnol.*, 2008, **28**, 277–284.
- 15 A. A. Aljabali, Y. Akkam, M. S. Al Zoubi, K. M. Al-Batayneh, B. Al-Trad, O. Abo Alrob, A. M. Alkilany, M. Benamara and D. J. Evans, *Nanomaterials*, 2018, **8**, 174.
- 16 M. Zheng, H. Jia, H. Wang, L. Liu, Z. He, Z. Zhang, W. Yang, L. Gao, X. Gao and F. Gao, *RSC Adv.*, 2021, **11**, 7129–7137.
- 17 S. Otari, R. Patil, S. Ghosh and S. Pawar, *Mater. Lett.*, 2014, **116**, 367–369.
- 18 C. Kamaraj, G. Rajakumar, A. A. Rahuman, K. Velayutham, A. Bagavan, A. Zahir and G. Elango, *J. Parasitol. Res.*, 2012, **111**, 2439–2448.
- 19 G. Rajakumar and A. A. Rahuman, *Res. Vet. Sci.*, 2012, **93**, 303–309.
- 20 B. Lin, Y. Zhao, P. Han, W. Yue, X.-Q. Ma, K. Rahman, C.-J. Zheng, L.-P. Qin and T. Han, *J. Ethnopharmacol.*, 2014, **155**, 248–255.
- 21 S. I. Ankier, *Eur. J. Pharmacol.*, 1974, **27**, 1–4.
- 22 J. Sedlak and R. H. Lindsay, *Anal. Biochem.*, 1968, **25**, 192–205.
- 23 H. Ohkawa, N. Ohishi and K. Yagi, *Anal. Biochem.*, 1979, **95**, 351–358.
- 24 A. K. Sinha, *Anal. Biochem.*, 1972, **47**, 389–394.
- 25 L. Magnani, E. M. Gaydou and J. C. Hubaud, *Anal. Chim. Acta*, 2000, **411**, 209–216.
- 26 I. B. McInnes and G. Schett, *N. Engl. J. Med.*, 2011, **365**, 2205–2219; J. Grand, P.-M. Adam, A.-S. Grimault, A. Vial, M. L. Chapelle, J.-L. Bijeon, S. Kostcheev and P. Royer, *Plasmonics*, 2006, **1**, 135–140.
- 27 J. Grand, M. Chapelle, J.-L. Bijeon, P.-M. Adam, A. Vial and P. Royer, *Phys. Rev. B: Condens. Matter Mater. Phys.*, 2005, **72**(3), 033407.
- 28 J. Grand, S. Kostcheev, J. L. Bijeon, L. Chapelle, P. M. Adam, A. Rumyantseva, G. Léronde and P. Royer, *Synth. Met.*, 2003, **139**, 621.
- 29 M. E. Weinblatt, E. C. Keystone, D. E. Furst, L. W. Moreland, M. H. Weisman, C. A. Birbara, L. A. Teoh, S. A. Fischkoff and E. K. Chartash, *Arthritis Rheum.*, 2003, **48**, 35–45.
- 30 R. W. Kinne, R. Bräuer, B. Stuhlmüller, E. Palombo-Kinne and G. R. Burmester, *Arthritis Res. Ther.*, 2000, **2**(3), 189.
- 31 M. Singh, P. Soni, N. Upmanyu and Y. Shivhare, *Asian J. Pharm. Tech.*, 2011, **1**(4), 123–124.
- 32 I. M. Chung, I. Park, K. Seung-Hyun, M. Thiruvengadam and G. Rajakumar, Plant-mediated synthesis of silver nanoparticles: their characteristic properties and therapeutic applications, *Nanoscale Res. Lett.*, 2016, **11**(1), 40.
- 33 X. Zhang, *Cell Biochem. Biophys.*, 2015, **72**(3), 771–775.
- 34 A. Ganguly, Z. Al Mahmud, M. M. N. Uddin and S. A. Rahman, *Asian Pac. J. Trop. Dis.*, 2013, **3**, 301–307.
- 35 R. W. Kinne, R. Bräuer, B. Stuhlmüller, E. Palombo-Kinne and G.-R. Burmester, *Arthritis Res. Ther.*, 2000, **2**, 1–14.
- 36 A. G. Mowat, *Semin. Arthritis Rheum.*, 1972, 195–219.
- 37 W. Grassi, R. De Angelis, G. Lamanna and C. Cervini, *Eur. J. Radiol.*, 1998, **27**, S18–S24.
- 38 S. S. Perumal, S. P. Ekambaram and T. Dhanam, *Pharm. Biol.*, 2017, **55**, 1330–1336.
- 39 A. Paradowska, W. Maśliński, A. Grzybowska-Kowalczyk and J. Łacki, *Arch. Immunol. Ther. Exp.*, 2007, **55**, 329.
- 40 K. Ashiq, M. A. Bajwa, S. Tanveer, M. Qayyum, S. Ashiq, R. Khokhar and F. A. Abid, *JPMA, J. Pak. Med. Assoc.*, 2021, 1–12.
- 41 A. Latif, K. Ashiq, S. Ashiq, E. Ali, I. Anwer and S. Qamar, *J. Anim. Plant Sci.*, 2020, **30**, 219–228.
- 42 P. R. Devi, S. K. Kumari and C. Kokilavani, *Indian J. Clin. Biochem.*, 2007, **22**, 143.
- 43 H. An, Z. Song, P. Li, G. Wang, B. Ma and X. Wang, *Appl. Nanosci.*, 2020, **10**(2), 617–622.

